Iranian Journal of Materials Forming 10 (1) (2023) 53-60

Online ISSN: 2383-0042

IJMF

Iranian Journal of Materials Forming

Journal Homepage: http://ijmf.shirazu.ac.ir

Research Article

The Simulation of Texture of $Al_{0.3}CoCrFeNi$ High Entropy Alloy after Cold Deformation using Visco-Plastic Self-Consistent Model

A.H. Hosseinifar* and K. Dehghani*

Department of Materials and Metallurgical Engineering, Amirkabir University of Technology (Tehran Polytechnic), Tehran, Iran

ARTICLE INFO

Article history:

Received 5 March 2023
Reviewed 19 April 2023
Revised 12 May 2023
Accepted 15 May 2023

Keywords:

Crystal plasticity
Cold rolling
High entropy alloys
Texture

Please cite this article as:

A.H. Hosseinifar, K. Dehghani, The simulation of texture of $Al_{0.3}CoCrFeNi$ High Entropy alloy after cold deformation using visco-plastic self-consistent model, *Iranian Journal of Materials Forming*, 10(1) (2023) 53-60.

ABSTRACT

In the present study, a visco-plastic self-consistent model (VPSC) was used to predict the $Al_{0.3}CoCrFeNi$ texture after cold rolling. The alloy under examination was produced via vacuum arc remelting and casting (VAR casting). Then, it was remelted four times to have the best structure homogeneity. However, the produced ingot was then homogenized at 1050°C for 10 h to remove the residual stress and reduce the micro-macro-segregation. This was followed by 75% cold reduction which was employed in seven passes. In order to simulate the $Al_{0.3}CoCrFeNi$ texture via the VPSC model, affine schemes and hardening parameters were used in this model. Moreover, this model was performed by Fortran 77 programming languages, and grain fragmentation and co-rotational effect were used in this code. In this study, a simulation process was used for 300 and 1000 grains. After that, simulation results were compared with experimental textures that were measured by the X-ray diffraction method. The results showed that both experimental and simulated textures have an acceptable compatibility. However, there are differences between the measured and simulated results, which can be attributed to the number of grains of estimated and simulated cases.

1. Introduction

High entropy alloys (HEAs) contain at least five principal elements at concentrations within the scope of 5-35% atomic percent. Different aspects of these alloys have been extensively investigated in the last decade due to their unique mechanical properties, such as high strength, great ductility, high abrasion resistance, corrosion resistance, etc. [1-4]. In addition, HEAs have strange properties such as high entropy, sluggish diffusion, severe lattice distortion, and cocktail effects. Some research in the field of HEAs show that FCC and BCC crystallographic structures are the major structures in HEAs [2].

Due to anisotropic elastic tensor and directional dependence of activation crystal deformation mechanism (dislocations, twins deformations, and martensite transformation), elastic-plastic deformation

* Corresponding authors
E-mail addresses: amirhosseinhosseinifar0@gmail.com (A.H. Hosseinifar), dehghani@aut.ac.ir (K. Dehghani)
https://doi.org/10.22099/IJMF.2023.46966.1253

behavior depends on load direction. So, crystals have anisotropic mechanical properties separately [5]. Therefore, crystal directions can express total anisotropic properties in a polycrystal material in the tensor's behavior of each grain and boundary conditions which depend on its inner crystal directions.

In case the distribution of grains is random, the materials will have texture. Hence, those materials which have texture are anisotropy, and their properties are different in each crystallographic direction. Hence, texture can have many effects on physical and mechanical properties [6]. There are several ways to measure textures, like XRD, TEM, and EBSD. XRD is used to measure macro-texture and other ways to measure micro-texture [7]. Besides, there are several ways like pole figure, inverse pole figure, and orientation distribution function (ODF) to show texture [8].

Polycrystal plasticities such as Taylor type [9] and the VPSC model [10] have been rigorously formulated and extensively used to understand and predict the texture of metals. The degree of complexity in crystal plasticity simulation depends on the number and type of deformation modes and crystal structures [11]. In this paper, we use $Al_{0.3}$CoCrFeNi with FCC crystal structure. This alloy is classified as a low stacking fault energy alloy, because its stacking fault energy is 20-25 MJ/m^2 [12, 13]. So, its deformation mechanism is the combination of slip systems and twins deformation [14].

Rolling is a mechanical process that makes anisotropic properties in materials. because in this process, grains extend in the rolling direction. Following the rolling process, materials have a preferred direction and anisotropic properties.

Mishin et al. [15] have focused on the effect of the cold rolling route on the deformation mechanism and texture evolution of thin beryllium foils by using the VPSC model. Despres et al. [11] have focused on the contribution of intergranular misorientation to the cold rolling textures of ferritic stainless steels using the VPSC model. Lebesohn and Tome [16] have predicted rolling textures of anisotropic polycrystals such as brass with FCC structure, zircaloy with HCP structure, calcite with trigonal structure, and uranium with orthorhombic structure.

In this paper, the experimental and numerical study of texture of $Al_{0.3}$CoCrFeNi high entropy alloy was evalualted by XRD and crystal plasticity. Besides, the effect of the number of grains on the accuracy of textures was studied.

2. Materials and Methods

2.1. Material and cold rolling parameters

Arc melting was used to prepare $Al_{0.3}$CoCrFeNi HEA ingot. Its chemical composition was of 3.254 wt.% Al, 25.435 wt.% Co, 22.825 wt.% Cr, 24.639 wt.% Fe, and 23.037 wt.% Ni, determined by XRF. Melting was carried out in a vacuum arc melting (VAR) furnace to minimize the contamination. Remelting was performed four times to ensure a homogenous chemical composition. Moreover, the homogenizing treatment was conducted at 1050°C for 10 h in a muffle furnace purged with argon gas. The homogenization temperature was carefully selected to avoid the formation of the second phase in $Al_{0.3}$CoCrFeNi HEA. This was based on the phase diagram developed by computational thermodynamics [17]. Cold rolling was then carried out on the homogenized alloy; the total 75% reduction was performed in seven passes, reaching the final thickness of 2 mm from 8 mm.

After each pass of rolling, the amount of the strain along the normal (ε_{ND}), rolling (ε_{RD}), and transverse (ε_{TD}) directions were measured to characterize the sample deformation [15]:

$$\varepsilon_{ND} = \ln\left(\frac{h_0}{h_1}\right) \quad (1)$$

h_0 and h_1 are the sample thickness before and after rolling, respectively.

$$\varepsilon_{RD} = \ln\left(\frac{l_1}{l_0}\right) \quad (2)$$

l_0 and l_1 are the sample length before and after rolling, respectively.

$$\varepsilon_{TD} = \ln\left(\frac{b_1}{b_0}\right) \quad (3)$$

b_0 and b_1 are the sample width before and after rolling, respectively.

XRD was carried out on all samples via a Philips Xpert machine using Cu-k_α radiation. The applied wavelength and diffraction angle were 1.542 Å and 2θ range of 30° to 100°, respectively. The XRD results are shown in Fig. 1. Then, the texture was measured by Philips PW1730 machine using Cu-k_α radiation for (111), (220), (200) planes in $0° < \alpha < 360°$, $0° < \beta < 90°$ with the step of 5°. Then, the results were processed by Philip texture software. Finally, the pole figures were determined after rolling, as are shown in Fig. 2.

2.2. Modeling texture evolution

In the present work, the VPSC model [10] was used to study the deformation mechanisms. In this model, each individual grain is modeled as an elliptical viscoplastic inclusion interacting with a homogeneous effective medium. This approach allows calculating the evolution of the crystallographic texture at each loading step.

The macroscopic response of a material predicted by a VPSC simulation depends on the linearization of the viscoplastic constitutive behaviors related to the individual grains [18]. There are different approaches for linearization, like secant, tangent, affine, and so on. These approaches can be implemented in the VPSC code [10, 19, 20].

The results of the VPSC modeling are closely related to the accuracy of the loading conditions settings. The velocity gradient tensor (L) must be defined to simulate rolling. Usually, this tensor is first calculated by Eq. (1) to Eq. (4) and then imported into the VPSC code to predict the texture evolution.

For the purpose of calculating the velocity gradient tensor, first, strains were calculated by Eq. (1) to Eq. (3). Afterward, the velocity of the gradient tensor was written using strain rate along the specified direction [15]:

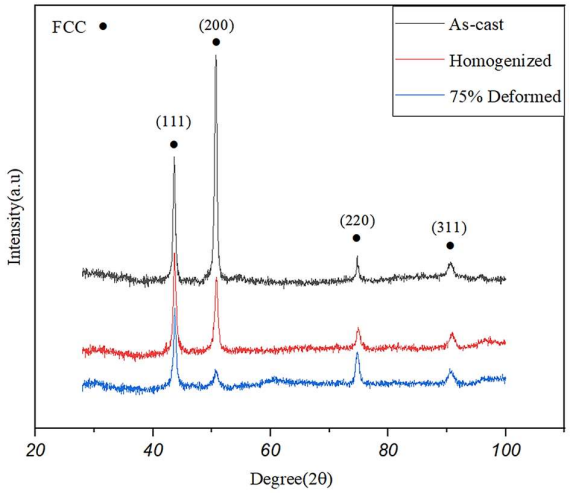

Fig. 1. XRD results after the casting and rolling process.

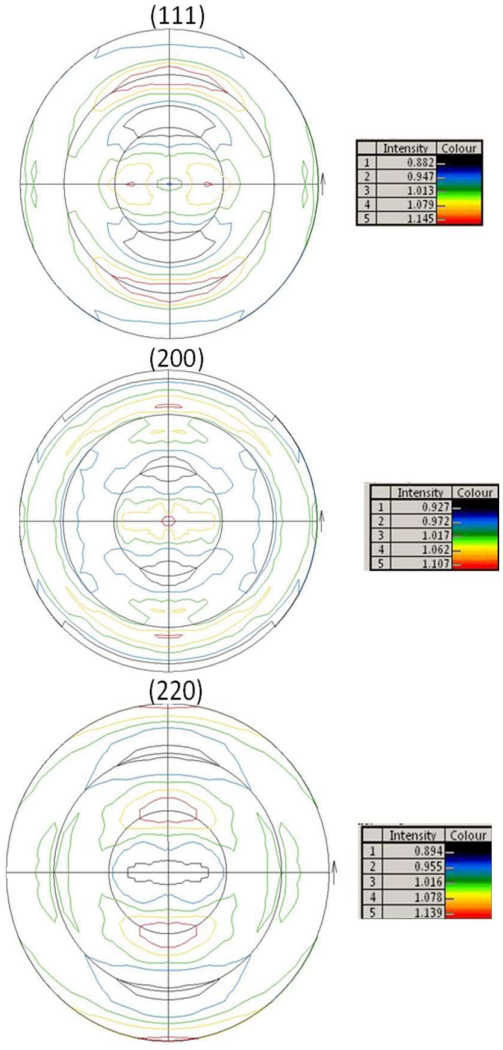

Fig. 2. Experimental pole figures for rolling sheet in the last pass of rolling.

$$L = \begin{bmatrix} \dot{\varepsilon}_{RD} & 0 & 0 \\ 0 & \dot{\varepsilon}_{TD} & 0 \\ 0 & 0 & -\dot{\varepsilon}_{ND} \end{bmatrix} \quad (4)$$

$\dot{\varepsilon}_{RD}$, $\dot{\varepsilon}_{TD}$, and $\dot{\varepsilon}_{ND}$ are strain rates in the RD, TD, and ND directions, respectively. Thus, this velocity gradient tensor was imported to the VPSC code to predict rolling texture.

The initial texture of an $Al_{0.3}$CoCrFeNi HEA after the homogeneous process was presented as a set of 1000 orientations. Then, experimentally measured strains in RD, TD, and ND were used to calculate the velocity of gradient and import in the VPSC model.

The value of the viscoplastic strain rate in grain was obtained using the following equation [21]:

$$\dot{\varepsilon} = \dot{\gamma}_0 \sum_s m_{ij}^s \left(\frac{m^s \sigma'}{\tau^s} \right)^n \quad (5)$$

where s, τ^s, m^s, σ', $\dot{\gamma}_0$ and n, are the slip or twining system, the threshold shear stress, the Schmid tensor for the grain, the Cauchy stress deviator, the normalization factor, and the strain rate sensitivity factor, respectively.

The strain rate sensitivity parameter n=15.87 was chosen according to Ref. [22] to resolve the activity in each system without ambiguity.

The threshold shear stress τ^s depends on the activities of deformation modes and was calculated by a modified Voce hardening equation [23]:

$$\tau^s = \tau_0^s + (\tau_1^s + \theta_1^s \times \Gamma) \left(1 - \exp\left(-\Gamma \left| \frac{\theta_0^s}{\tau_1^s} \right| \right) \right) \quad (6)$$

where s is the slip or twining system, Γ is the cumulative shear deformation in a grain, τ_0^s and $(\tau_0^s+\tau_1^s)$ are the initial and back extrapolated critical resolved shear stress (CRSS), θ_0^s and θ_1^s are the hardening parameters.

Based on previous research [24], effective Schmid factors were calculated for slip and twin systems. So, based on the effective Schmid factor approach, if τ^s is equal to CRSS, the slip system is active. In FCC materials, there are 12 slip systems, so there are 12 τ^s to be compared with CRSS. Hence, this approach was done for twin systems.

The model can be validated by comparing the calculated and experimental rolling textures. As a rule, the parameters are determined by fitting multi-directional stress-strain curves [25-27]. For $Al_{0.3}$CoCrFeNi HEA's rolled sheets, it is possible to perform tensile tests. Therefore, experimentally obtained textures were used to determine the model fitting parameters. After the VPSC simulation, the resultant set of orientations was used for ODF estimation in Fortran code. The complete pole figures were recalculated from ODF, allowing a quantitative comparison of the calculated textures with the experimental ones.

Based on the previous research [16], different choices are possible for linearized behavior at the grain level in a way that eventually, the results of the self-consistent scheme depend on this choice. In this study, the affine linearization scheme was implemented in the VPSC code because, among other linearization schemes, due to being more reliable and accurate.

The CRSS values and hardening parameters for $Al_{0.3}$CoCrFeNi at room temperature initially taken from [28] had to be modified for a better agreement between the calculated and experimental textures (see Table 1).

Table 1. Simulation parameters used for this study

Scheme	n	τ_0	τ_1	θ_0	θ_1	$h_{ss'}$
Affine	15.87	98.3	128	900	0	1

In addition to the orientations of grains after cold rolling, the activities of the slip systems and twinning were obtained as a function of the accumulated strain in our VPSC simulations.

3. Results and Discussion

3.1. XRD results

One of the characteristics of HEAs is the high entropy which causes the formation of solid solution either with FCC and BCC as well as the combination of the both. In such a case, a number of solute elements are present in the matrix during solidification [29-31].

According to the XRD results presented in Fig. 2, the crystal structure for $Al_{0.3}$CoCrFeNi HEA after casting,

homogenizing, and rolling is FCC. Thus, homogenizing and the rolling process have not changed the casting crystal structure. Based on previous research [31], the homogenization temperature was carefully selected to avoid the formation of the second phase. Also, the effect of deformation percentage on the formation of second phases or precipitates is very insignificant. Therefore, no change in the crystal structure occurred during the rolling process, because there was no second phase or precipitates.

According to Fig. 1, the rolling process results in inhomogeneity in the rolling sheet. That is because after rolling, the grains were elongated in the rolling direction; consequently, the distribution of grains is not random.

3.2. VPSC simulation

Before simulating the texture and before attaining the pole figures by VPSC model and crystal plasticity approach, the following steps were taken: I) extracting deformation history, II) importation velocity gradients for each step in Fortran code, and III) importation hardening parameters, slip and twin system and other parameters being explained in the previous part.

It is expected that the reorientation of grain during deformation will be affected to some extent by the neighboring grains. Specifically, if neighboring grains exhibit different reorientation trends, they can be expected to drag each other. An empirically simple way of accounting for such effect inside VPSC is to assign a neighbor at random to every grain, to calculate the spin of each grain, to average the spin of the two randomly paired grains, and to assign this average spin to each of them. This is the co-rotational effect. As a result of this procedure, grains with the same initial orientation will reorient differently during deformation because each of them will interact with a different neighbor [16].

Under severe plastic deformation, grains adopt distorted shapes and extreme aspect ratios and tend to rotate with the flow field at a faster rate than equiaxed grains. However, there are physical and numerical limits to how distorted a grain can become. From a physical point of view, severely distorted grains are likely to split into sub-grains. This is the grain fragmentation effect [10].

In the present simulation, the initial texture was considered to have 1000 grains; where grain fragmentation and co-rotational grain were used as well.

When polycrystals undergo plastic deformation, the deformation in each grain should be compatible with neighbor grains. This is so-called compatibility deformation. Therefore, the co-rotational process provides the compatible deformation condition in the VPSC model. Consequently, every two ellipsoid grains, which are paired, rotate in a way that satisfies the compatible deformation condition. Fig. 3 shows the pole figures after the last pass of rolling obtained experimental as well as by simulation. According to Fig. 3, the pole figures obtained by simulation and experimental exhibit good conformity in terms of their appearance. In both pole figures, most of the grains have a preferred direction and are elongated to the RD direction. Note that the vertical axis is RD direction and the horizontal axis is TD direction. Previous research [33] indicated that the differences between simulation and experimental pole figures are related to the VPSC model and the number of grains. In the VPSC model, only a part of intergranular interaction is investigated, whereas short-range and long-range interactions are not investigated. Thus, in the VPSC model, all of the interactions for grains are not investigated [33]. As already mentioned, the number of grains can affect the final texture.

Referring to the pole figures presented in Fig. 3, each grain is shown by three points, indicating the rotation of crystals around the TD, ND, and RD axes. Thus, decreasing the number of grains causes the rotation of all grains to not appear in the simulated pole figures compared to the experimental pole figures. Therefore, the simulation process was performed for 300 and 1000 grains and compared with experimental textures. Fig. 4 compares the pole figures for the 300 and 1000 grains with experimental textures.

Therefore, the number of grains is the main factor in crystal plasticity simulation, that is because the number of grains can affect the formation of components and their intensity in textures.

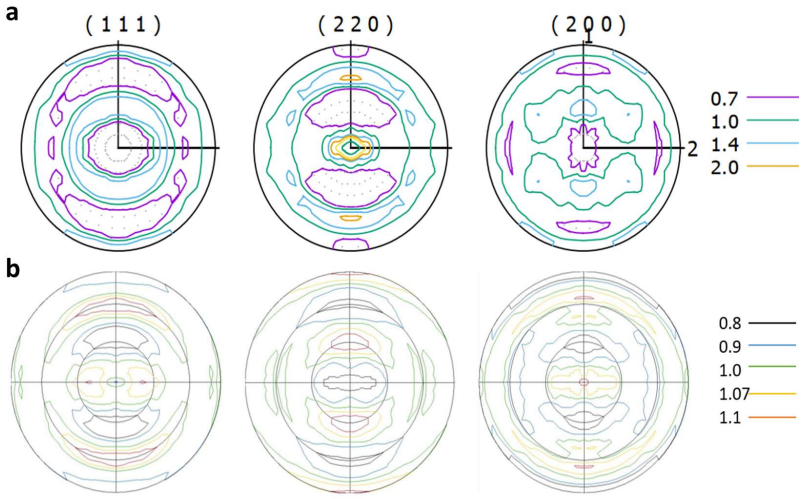

Fig. 3. Pole figures for (a) simulation by VPSC model, and (b) experimental by XRD.

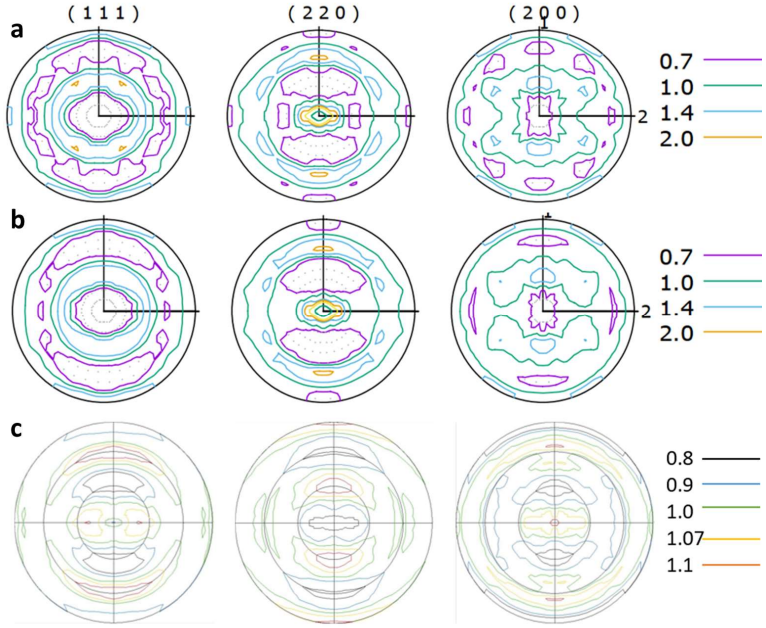

Fig. 4. Pole figures for (a) 300 grains, (b) 1000 grains, and (c) experimental.

4. Conclusion

In the present paper, after the cold rolling of $Al_{0.3}CoCrFeNi$ HEA, the texture evolution was investigated by experiments and modeling. Using the VPSC model, the crystallographic texture of $Al_{0.3}CoCrFeNi$ was predicted. The main conclusions can be summarized as follow:

1. The crystallographic structure was FCC for the casting and rolling process. Thus, the rolling process does not change the casting's crystal structure.
2. The texture that the VPCS model predicted is compatible with the experimental texture.
3. The main reason for the difference in simulated texture in experimental texture is the number of grains. If the number of grains increases, the simulated texture is more reliable.

Acknowledgments

The authors appreciate the members of the Material Science laboratory of Amirkabir University of Technology for their help and support to carry out simulation process and experiments.

Conflict of Interests

The authors declare no conflict of interest.

Funding

This research did not receive any specific funding.

5. References

[1] J.W. Yeh, S.K. Chen, S.J. Lin, J.Y. Gan, T.S. Chin, T.T. Shun, C.H. Tsau, S.Y. Chang, Nanostructured high entropy alloys with multiple principal elements: novel alloy design concepts and outcomes, *Advanced Engineering Materials*, 6(5) (2004) 299-303.

[2] Y. Zhang, T.T. Zuo, Z. Tang, M.C. Gao, K.A. Dahmen, P.K. Liaw, Z.P. Lu, Microstructures and properties of high-entropy alloys, *Progress in Materials Science*, 61 (2014) 1-93.

[3] A.J. Zaddach, R.O. Scattergood, C.C. Koch, Tensile properties of low-stacking fault energy high-entropy alloys, *Materials Science and Engineering: A*, 636 (2015) 373-378.

[4] D. Li, C. Li, T. Feng, Y. Zhang, G. Sha, J.J. Lewandowski, P.K. Liaw, Y. Zhang, High-entropy $Al_{0.3}CoCrFeNi$ alloy fibers with high tensile strength and ductility at ambient and cryogenic temperatures, *Acta Materialia*, 123 (2017) 285-294.

[5] F. Roters, P. Eisenlohr, T.R. Bieler, D. Raabe, Crystal plasticity finite element methods: in Materials science and engineering, John Wiley & Sons, Weinheim, 2011.

[6] K.D. Liss, A. Bartels, A. Schreyer, High-energy X-rays: a tool for advanced bulk investigations in materials science and physics, *Textures and Microstructures*, 35(3-4) (2003) 219-252.

[7] H.R. Wenk, P. Van Houtte, Texture and anisotropy, Reports on Progress in Physics, 67(8) (2004) 1367.

[8] H. Hu, Texture of metals, *Texture*, 1 (1974) 233-258.

[9] G.I. Taylor, Plastic strain in metals, *Journal of the Institute of Metals*, 62 (1938) 307-324.

[10] R.A. Lebensohn and C.N. Tomé, A self-consistent anisotropic approach for the simulation of plastic deformation and texture development of polycrystals: application to zirconium alloys, *Acta Metallurgica et Materialia*, 41(9) (1993) 2611-2624.

[11] A. Despres, M. Zecevic, R.A. Lebenson, J.D. Mithieux, Contribution of intragranular misorientation to the cold rolling textures of ferritic stainless steels, *Acta Materialia*, 182 (2020) 184-196.

[12] A.J. Zaddach, C. Niu, C.C. Koch, D.L. Irving, Mechanical properties and stacking fault energies of NiFeCrCoMn high-entropy alloy, *JOM*, 65 (2013) 1780-1789.

[13] N. Kumar, Q. Ying, X. Nie, R.S. Mishra, Z. Tang, P.K. Liaw, R.E. Brennan, K.J. Doherty, K.C. Cho, High strain-rate compressive deformation behavior of the $Al_{0.1}CrFeCoNi$ high entropy alloy, *Materials & Design*, 86 (2015) 598-602.

[14] M. Annasamy, N. Haghdadi, A. Taylor, P. Hodgson, D. Fabijanic, Static recrystallization and grain growth behavior of Al0.3CoCrFeNi high entropy alloy, *Materials Science and Engineering: A*, 754 (2019) 282-294.

[15] V.V. Mishin, I.A. Shishov, O.N. Stolyarov, I.A. Kasatkin, Effect of cold rolling route on deformation mechanism and texture evolution of thin beryllium foils: exprement and VPSC simulation, *Materials Characterization*, 164 (2020) 110350.

[16] R.A. Lebensohn, C. Tomé, A self-consistent viscoplastic model: prediction of rolling textures of anisotropic polycrystals, *Materials Science and Engineering: A*, 175(1-2) (1994) 71-82.

[17] C. Zhang, F. Zhang, S. Chen, W. Cao, Computational thermodynamics aided high-entropy alloy design, *JOM*, 64 (2012) 839-845.

[18] R.A. Lebensohn, C.N. Tomé, P.J. Maudlin, A selfconsistent formulation for the prediction of the anisotropic behavior of viscoplastic polycrystals with voids, *Journal of the Mechanics and Physics of Solids*, 52(2) (2004) 249-278.

[19] J.W. Hutchinson, Bounds and self-consistent estimates for creep of polycrystalline materials, *Proceedings of the Royal Society of London. A. Mathematical and Physical Sciences*, 348 (1976) 101‑127.

[20] R. Masson, M. Bornert, P. Suquet, A. Zaoui, An affine formulation for the prediction of the effective properties of nonlinear composites and polycrystals, *Journal of the Mechanics and Physics of Solids*, 48(6-7) (2000) 1203-1227.

[21] C.N. Tomé, P.J. Maudlin, R.A. Lebensohn, and G.C. Kaschner, Mechanical response of zirconium—I. Derivation of a polycrystal constitutive law and finite element analysis, *Acta Materialia*, 49(15) (2001) 3085-3096.

[22] S. Gangireddy, B. Gwalani, K. Liu, R. Banerjee, R.S. Mishra, Microstructures with extraordinary dynamic

work hardening and strain rate sensitivity in $Al_{0.3}$CoCrFeNi high entropy alloy, *Journal of Materials Science and Engineering: A*, 734 (2018) 42-50.

[23] M.A. Iadicola, L. Hu, A.D. Rollett, T. Foecke, Crystal plasticity analysis of constitutive behavior of 5754 aluminum sheet deformed along bi-linear strain paths, *International Journal of Solids and Structures*, 49(25) (2012) 3507-3516.

[24] S.F. Chen, H.W. Song, S.H. Zhang, M. Cheng, C. Zheng, M.G. Lee, An effective Schmid factor in consideration of combined normal and shear stress for slip/twin variant selection of Mg-3Al-1Zn alloy, *Scripta Materialia*, 167 (2019) 51-55.

[25] A. Chapuis, Z.Q. Wang, Q. Liu, Influence of material parameters on modeling plastic deformation of Mg alloys, *Materials Science and Engineering: A*, 655 (2016) 244-250.

[26] J. Galán-López, P. Verleysen, Simulation of the plastic response of Ti–6Al–4V thin sheet under different loading conditions using the viscoplastic self-consistent model, *Materials Science and Engineering: A*, 712 (2018) 1-11.

[27] H. Pan, F. Wang, M. Feng, L. Jin, J. Dong, P. Wu, Mechanical behavior and microstructural evolution in rolled Mg-3Al-1Zn-0.5Mn alloy under large strain simpleshear, *Materials Science and Engineering: A*, 712 (2018) 585-591.

[28] Q. Jiao, G.D. Sim, M. Komarasamy, R.S. Mishra, P.K. Liaw, J.A. El-Awady, Thermo-mechanical response of single-phase face centered cubic Al_xCoCrFeNi high entropy alloy microcrystals, *Materials Research Letters*, 6(5) (2018) 300-306.

[29] J.W. Yeh, S.K. Chen, S.J. Lin, J.Y. Gan, T.S. Chin, T.T. Shun, C.H. Tsau, S.Y. Chang, Nanostructured high entropy alloys with multiple principal elements: Novel alloy design concepts and outcomes, *Advanced Engineering Materials*, 6(5) (2004) 299-303.

[30] J.W. Yeh, S.J. Lin, T.S. Chin, J.Y. Gan, S.K. Chen, T.T. Shun, C.H. Tsau, S.Y. Chou, Formation of simple crystal structures in Cu-Co-Ni-Cr-Al-Fe-Ti-V alloys with multiprincipal metallic elements, *Metallurgical and Materials Transactions A*, 35 (2004), 2533-2536.

[31] Y. Zhang, Y.J. Zhou, J.P. Lin, G.L. Chen, P.K. Liaw, Solid-solution phase formation rules for component alloys, *Advanced Engineering Materials*, 10(6) (2008) 534-538.

[32] Y.J. Zhou, Y. Zhang, F.J. Wang, G.L. Chen, Phase transformation induced by lattice distortion in multiprincipal component Co Cr Fe Ni Cu_x Al_{1-x} solid-solution alloys, *Applied Physics Letters*, 92(24) (2008) 241917.

[33] A. Khajezadeh, M. Habibi Parsa, H. Mirzadeh, Crystal plasticity analysis of texture evolution of pure aluminum during processing by a new severe plastic deformation technique, *Metallurgical and Materials Transactions A*, 47 (2016) 941-948.